The Journal of Chemical Physics

Optimizing dynamical functions for speed with stochastic paths

Cite as: J. Chem. Phys. **157**, 224101 (2022); https://doi.org/10.1063/5.0125479
Submitted: 12 September 2022 • Accepted: 18 November 2022 • Published Online: 08 December 2022

Rebecca A. Bone and Jason R. Green

The Journal of Chemical Physics ARTICLE scitation.org/journal/jcp

Optimizing dynamical functions for speed with stochastic paths

Cite as: J. Chem. Phys. 157, 224101 (2022); doi: 10.1063/5.0125479
Submitted: 12 September 2022 • Accepted: 18 November 2022 •
Published Online: 8 December 2022

Rebecca A. Bone[1] and Jason R. Green[1,2,a)]

AFFILIATIONS

[1] Department of Chemistry, University of Massachusetts Boston, Boston, Massachusetts 02125, USA
[2] Department of Physics, University of Massachusetts Boston, Boston, Massachusetts 02125, USA

[a)] **Author to whom correspondence should be addressed:** jason.green@umb.edu

ABSTRACT

Living systems are built from microscopic components that function dynamically; they generate work with molecular motors, assemble and disassemble structures such as microtubules, keep time with circadian clocks, and catalyze the replication of DNA. How do we implement these functions in synthetic nanostructured materials to execute them before the onset of dissipative losses? Answering this question requires a quantitative understanding of when we can improve performance and speed while minimizing the dissipative losses associated with operating in a fluctuating environment. Here, we show that there are four modalities for optimizing dynamical functions that can guide the design of nanoscale systems. We analyze Markov models that span the design space: a clock, ratchet, replicator, and self-assembling system. Using stochastic thermodynamics and an exact expression for path probabilities, we classify these models of dynamical functions based on the correlation of speed with dissipation and with the chosen performance metric. We also analyze random networks to identify the model features that affect their classification and the optimization of their functionality. Overall, our results show that the possible nonequilibrium paths can determine our ability to optimize the performance of dynamical functions, despite ever-present dissipation, when there is a need for speed.

I. INTRODUCTION

Synthetic and biological systems can perform *dynamical functions*.[1,2] These functions include the assembly[3–5] and replication[6] of structure, keeping of time,[7] and generation of work.[8] For example, biological motor proteins transport nutrients along microtubules, accomplishing their work on precise timescales in order to sustain cell functions.[9] ATP fuels the motive force of hauling cellular cargo, despite the dissipative loss of energy as heat, with the speed required to sustain cellular life. Synthetic materials are now being driven out of equilibrium to quickly execute these dynamical functions: outputting work,[10] self-replicating,[11] and self-destroying.[12,13] Recent experiments on responsive materials[14] suggest the potential to tune environmental stimuli[15] that speed up or slow down these processes. However, it is unclear how to balance speed against performance and the dissipation of entropy or heat, making it a challenge to optimize the functionality.

Exacerbating this challenge to the design of nanoscale systems is that the fluctuations of their dissipative processes can be comparable in magnitude to the motions executing the function. While the principles of thermodynamics meet our need to optimize the energy efficiency of slow-moving macroscopic matter, they do not readily translate to these practically important fast-moving, stochastic materials.[16] One way to overcome this challenge could be to create systems that can deliver work or high-yield structures on timescales that are shorter than those of entropic losses. However, is this type of process possible for a given system? Implementing this design feature requires a detailed understanding of how the speed of stochastic paths correlates with dissipation[17] and the function performance. We address this question here by mapping the design space for optimization and establishing a protocol for assigning a given model to a particular functional modality. These steps enable us to classify the potential to optimize dynamical functions over finite timescales, despite their stochastic and dissipative nature.

To measure the thermodynamic costs and benefits of dynamical functionality, we adopt the framework of stochastic thermodynamics,[18,19] which has established measures of dissipation

for individual stochastic paths.[20–22] Recent work in this area led to thermodynamic speed limits on observables which are global bounds on speed and dissipation.[23–25] Some of these[25] combine with the time-energy uncertainty relation to give general speed limits on open quantum systems.[26] (In fact, their quantum analog, the time-energy uncertainty relation, has been used as a design principle for synthetic molecular motors.[27]) These bounds on the speed of dissipation rates suggest the need for a closer analysis of the relationships between these variables for stochastic paths.

Taking up this analysis here, we show how to classify dynamical functions based on whether the speed, dissipation, and performance can be simultaneously optimized by tuning experimentally controllable parameters, such as temperature, pH, and potential difference. We map the design space using stochastic paths, identifying four distinct optimization modalities, Fig. 1. This categorization suggests a protocol to determine our ability to optimize the performance of models for dynamically functioning systems. Applying this protocol to both known and random models shows that in only one mode are there high-performing paths that can occur sufficiently quickly to avoid dissipative losses.

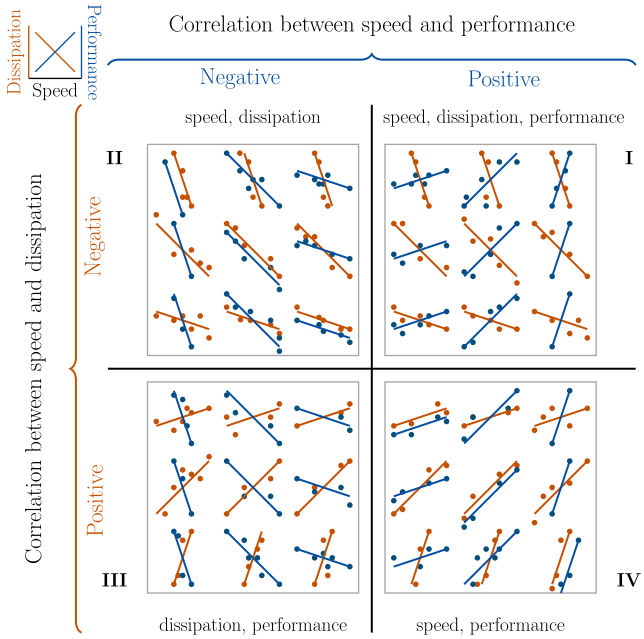

FIG. 1. Design space of dynamical function: Schematic illustration of four optimization modalities for dynamical functions from the perspective of stochastic path observables. Each quadrant shows representative datasets for the dissipation (orange) and the performance metric (blue) as a function of the path speed across an ensemble of stochastic paths that execute a function: timekeeping, structure formation or replication, and work generation. The correlation between speed and performance (blue), together with the correlation between speed and dissipation (orange), across these stochastic paths, maps the design space. The observables that can be simultaneously optimized label each regime. In **I**, faster paths enhance performance and suppress dissipative losses. In **II**, slower paths enhance performance but also increase dissipative losses. In **III**, slower paths enhance performance and suppress dissipative losses. In **IV**, faster paths enhance performance but also increase dissipative losses.

II. PROTOCOL FOR CLASSIFYING MODELS OF DYNAMICAL FUNCTION

Can we modulate external conditions to simultaneously optimize speed, dissipation, and the performance metric for a particular model of a system that functions dynamically? To answer this question with stochastic paths, there are five steps we take to assign a model to a particular optimization mode.

A. Input Markov model for dynamical function

As input, we take a discrete-state, continuous-time Markov model that consists of a set of N states, $x = 1, 2, \ldots, N$. The master equation governs the dynamics,[28]

$$\frac{d}{dt}p(x,t) = \sum_{y\neq x}^{N}[w(x|y)p(y,t) - w_x p(x,t)], \tag{1}$$

with time–homogeneous transition rates $w(x|y)$ between any two states x and y, determining the temporal evolution of the probability distribution over model states.[28] The second term includes the escape rate, $w_x = \sum_{y\neq x}^{N} w(y|x)$, from x. One solution of the master equation expresses the marginal probabilities, $p(x,t)$, as a sum over paths,[20,21,29]

$$p(x_f,t) = \sum_{n=0}^{\infty}\sum_{\mathcal{C}_n}\mu(\mathcal{C}_n = x_0, x_1, \ldots, x_f, t), \tag{2}$$

which accounts for the joint probability, $\mu(\mathcal{C}_n, t)$, of visiting all the possible paths, $x_0, x_1, \ldots, x_f$, that the system can take through the physical states that end in $x = x_f$ at time t.

B. Sample or enumerate stochastic paths

We will distinguish between the terms *path* and *trajectory*. A *path* is a series of time-ordered states, $\mathcal{C}_n := x_0, x_1, \ldots, x_{n-1}, x_n$. A trajectory is a series of time-ordered states and the associated times when the system transitions to each state, $\mathcal{T}_n := x_0, t_0; x_1, t_1; \ldots; x_{n-1}, t_{n-1}; x_n, t_n$. Many trajectories will follow the same path with different sequences of transition times. Our focus here is on the stochastic paths that transition between an initial and final state in a given amount of time, t. Each model here has a clear initial, x_0, and final, x_f, state associated with a particular function, so we only generate stochastic paths between these fixed endpoints.

Given the initial and final states, different numerical approaches are available to generate a set of paths. For shorter paths, we can generate the entire ensemble by brute-force enumeration. For longer paths, other approaches, such as sampling with kinetic Monte Carlo,[28] are necessary. Here, we explicitly enumerate sequences of states for a chosen number of state-to-state transitions n between the initial and final states. We find all paths of each length n up to a maximum length $n_{\max}$. To minimize some of the computational expense, the enumeration accounts for whether a transition from state x_i to x_{i+1} is possible; in increasing the path length by one transition, we only add states for which there is a nonzero transition rate in the input model. The maximum length of paths we use is $n_{\max} = 22$ for the clock, 20 for the ratchet, 17 for self-assembly, and 15 for the copier.

C. Compute probabilities for stochastic paths

Paths in the chosen ensemble can vary in the time they take to execute a function, the amount of energy and entropy they dissipate, and the probability of their occurrence.[3,30–32] To identify which paths, among the myriad, deliver the desired work, yield, or precision in a desired amount of time, we use the contracted path probability, $\mu(\mathcal{C}_n, t)$.[17] This probability is the exact, closed-form expression for the joint probability, $\mu(\mathcal{C}_n, t)$, that the system takes a path $\mathcal{C}_n$ of n jumps that ends in x_f after time t. It has contributions from all trajectories following the path that complete within the time t. From Bayes' rule, it is the product

$$\mu(\mathcal{C}_n, t) = p(\mathcal{C}_n)p(t|\mathcal{C}_n) \tag{3}$$

of the probability of a path,

$$p(\mathcal{C}_n) = p(x_0, t_0)\prod_{i=1}^{n} \frac{w(x_i|x_{i-1})}{w_{x_{i-1}}}, \tag{4}$$

and the probability that path will complete within time t,

$$p(t|\mathcal{C}_n) = \rho_0 * \left[\rho_1 * \left[\rho_2 * \left[\cdots * \rho_{n-1} * e^{-w_{x_n}(t-t_n)}\right]\right]\right], \tag{5}$$

which is the convolution of each of the exponentially-distributed waiting time distributions. The last exponential factor is the survival probability in the final state. The waiting time, $\Delta t_i = t_{i+1} - t_i$, in each state x_i along the path is exponentially distributed,

$$\rho(\Delta t_i) = \rho_i = w_{x_i} e^{-w_{x_i}\Delta t_i}, \tag{6}$$

with respect to the escape rate from that state, w_{x_i}.

Evaluating the convolutions is a challenge, in part because the escape rates along a particular path can be degenerate. Others have shown that the contracted path probability is a sum of partial derivatives[21] with respect to the unique escape rates. We recently derived the closed-form expression,[17]

$$\mu(\mathcal{C}_n, t) = p(x_0, t_0)\prod_{i=1}^{n} w(x_i|x_{i-1})\sum_{j=1}^{n'} \frac{(-1)^{m_j-1}}{(m_j-1)!} \frac{e^{-w_{x_j}t}}{\prod_{\substack{k=1\\k\neq j}}^{n'} (w_{x_k} - w_{x_j})^{m_k}}$$
$$\times \sum_{l=1}^{m_j} \binom{m_j - 1}{l-1} (-t)^{m_j-l} d_j^{(l-1)}, \tag{7}$$

accounting for the n' unique escape rates, each with a degeneracy or number of occurrences m_j along the path. The function $d_j^{(l-1)}$ represents the mixing of the derivative terms resulting from the nested convolutions of the waiting time distributions. Jupyter notebooks are available online[33] with minimal working implementations of this formula and known simplifications.

D. Compute observables for stochastic paths

With this contracted path probability, we can determine a variety of observables and their moments: measures of speed, dissipation, and performance for model systems accomplishing a dynamical function. With these observables, we can then assess the quality of that dynamical function as a basis for optimization.

The observables common to all of our models of dynamical functions are "speed" and dissipation. Because the waiting times along a path are independent and exponentially distributed, the mean time to traverse a path is the sum of the mean waiting times in each state,[20]

$$\langle\tau\rangle_{\mathcal{C}_n} = \sum_{i=0}^{n} w_{x_i}^{-1}. \tag{8}$$

This path occurrence time is an intrinsic measure of the average time it will take for a system to follow a given path. Here, we calculate the contracted path probability at the mean path occurrence time $\langle\tau\rangle_{\mathcal{C}_n}$[17,33] and define the speed of a path by the inverse of the path occurrence time, $1/\langle\tau\rangle_{\mathcal{C}_n}$. This observable measures how quickly a path completes as an average over possible waiting times in each state.

Stochastic thermodynamics has measures of the dissipation associated with the trajectories taking a particular path: the entropy flow and entropy production.[18,19] The entropy production,

$$\frac{s_i[\mathcal{C}_n]}{k_B} = -\ln\frac{p(x_n, t)}{p(x_0, t_0)} - \ln\frac{\prod_{i=1}^{n} w(x_{i-1}|x_i)}{\prod_{i=1}^{n} w(x_i|x_{i-1})}, \tag{9}$$

is the amount of entropy produced by the system. The entropy flow,

$$\frac{s_e[\mathcal{C}_n]}{k_B} = -\ln\prod_{i=1}^{n}\frac{w(x_i|x_{i-1})}{w(x_{i-1}|x_i)}, \tag{10}$$

is the amount of entropy produced by the surroundings.[18] If all transition rates are exponentially related to the energy, $w(x_j|x_i) \propto Ae^{-\beta\Delta\epsilon}$, the entropy flow also gives the heat dissipated,[34] $q[\mathcal{C}_n] = -k_BTs_e[\mathcal{C}_n]$. We measure the entropy dissipated by the system to the surroundings with the negative of the entropy flow, $-s_e[\mathcal{C}_n]/k_B$.

Each history of the stochastic processes we consider executes a dynamical function. To quantitatively assess these functions, we choose an appropriate performance metric, such as timekeeping precision, the amount of work generated, or the yield of a desired structure. We average these observables, as well as measures of dissipation and speed, for each path using uniform-length time windows. We include paths in a window if their mean occurrence time falls within $t \leq \langle\tau\rangle_{\mathcal{C}_n} \leq t + \Delta t$. Averaging an observable, $\mathcal{O}$, within each time window,

$$\langle\mathcal{O}\rangle_t = \sum_{t}^{t+\Delta t} \mathcal{O}_{\mathcal{C}_n}\mu(\mathcal{C}_n, \langle\tau\rangle_{\mathcal{C}_n}), \tag{11}$$

produces a series of time-ordered observable values. The choice of time window size should give a time series, $\langle\mathcal{O}\rangle_t$, for each observable that is reasonably smooth to identify clear correlations between speed/dissipation and between speed/performance. Here, we varied the length of time windows Δt to find a value that showed a clear trend in observables without significant discreteness. The time window sizes we used here depended on the parameter values for each model, but they were generally around 0.1–2. We also average observables over all paths of length $0 \leq n \leq n_{\max}$,

$$\langle\mathcal{O}\rangle = \sum_{n=0}^{n_{\max}}\sum_{\mathcal{C}_n}\mathcal{O}_{\mathcal{C}_n}\mu(\mathcal{C}_n, \langle\tau\rangle_{\mathcal{C}_n}). \tag{12}$$

We scan all the parameters of each model to analyze their effect on these ensemble averages: positive valued parameters over $0.1, 0.2, \ldots, 1, 2, \ldots, 10$ and negative valued parameters over $-0.1, -0.2, \ldots, -1, -2, \ldots, -10$. The only exceptions were the copier-model parameters δ, which we vary over $\delta \in [0.7, 6]$, and ϵ, which we vary over $\epsilon \in [20, 100]$.

E. Output assignment of optimization mode

The final step of this protocol is to output an assignment of the optimization mode of the model. Our objective is to determine whether the system following faster stochastic paths improves the performance metric and the associated dissipation. Given measures of speed, dissipation, and performance for the input model, we average each observable over an ensemble of stochastic paths in fixed time intervals, Δt. To assign the optimization mode, we analyze the pairwise correlation of speed with the performance metric and speed with dissipation over time. As illustrated in Fig. 1, we use these correlations to assign each model to a particular modality (**I**–**IV**), with each modality representing how we can optimize its functional performance. From our survey of models for dynamical function, all four combinations of positive and negative correlations are possible. The exact modality depends on the positivity or negativity of the correlation, regardless of its linearity or the strength of the correlation, between the speed and the dissipation and between the speed and the performance metric.

III. FOUR OPTIMIZATION MODES OF DYNAMICAL FUNCTION MODELS

We demonstrate the protocol with Markov models for dynamical functions. The first we will discuss are four representative models from Ref. 1: a clock for timekeeping, a ratchet for generating work, a copier capable of self-replication, and a system that self-assembles into a desired structure.[33] Each of these dynamical functions has a natural measure of performance. The clock measures time with a certain precision, the ratchet outputs useful work in discrete increments, the self-assembling system generates a certain yield of fully assembled structures, and the replicator creates a correct copy with a certain yield. Jupyter notebooks demonstrating the protocol for these models of dynamical function are available online.[33] We find that each of these models belongs to a different optimization mode.

A. Faster stochastic paths enhance performance and suppress dissipative losses

In constructing artificial molecular motors, for example, a particularly desirable mode of function is one in which speeding up the process improves the delivery of work and simultaneously suppresses dissipative losses.[35] In this case, one could design systems to execute tasks quickly with high efficiency by evolving along stochastic paths in which speed negatively correlates with dissipation and positively correlates with performance, Fig. 1.

As a representative application of our protocol, we analyzed the timekeeping ability of a model electromechanical oscillator.[1] The state diagram of this four-state Markov model is in Fig. 2(a). Physically, the system keeps time by oscillating a particle between two electrodes.[7,36] Two states in the model represent when the particle is at the first electrode, and two states represent when it is at the second electrode; in each pair of states, the particle has either the same or opposite charge as the electrode. The model also captures the two types of possible transitions: physical translocation and charge change. The rates of charge transfer, k_c, and physical translocation, k_m, in the electrostatically favored direction are $k_c e^{F-A/2}$ and $k_m e^{-F}$ in the electrostatically unfavorable direction. The energy difference between electrodes F and the affinity, $A = 2\beta\text{eV}$, where $\beta = 1/k_B T$ and eV is electron affinity, act as barriers to transitioning in the electrostatically unfavorable direction (a particle moving to an electrode of the same charge as the particle).

The objective when physically implementing a timekeeping device is to select a kinetics that keeps time with high resolution (each "tick" occurs at a high speed), high precision (each tick is of approximately the same length), and minimal dissipative losses (the operating cost is low). Our ability to resolve time in the model, to resolve each "tick," and to measure it precisely depends on the distribution of occurrence times of stochastic paths. Each "tick" of the model clock corresponds to the set of fixed-endpoint paths that start and end in state 1; that is, each tick of the clock corresponds to a path completing one revolution around the cycle, $x_0 = x_f = 1$. Each time the particle returns to a designated "first" electrode marks one unit of time.

From the perspective of the stochastic paths, high-resolution timekeeping (short intervals of time) requires fast paths in the Markov model. Our measure of resolution is $\langle \tau \rangle_t$. Our measure of precision is the inverse of the relative variance of the mean occurrence time $\langle \tau \rangle_t^2 / \sigma_t^2(\tau)$, which is similar to measures used to analyze other classical clocks.[1,37] We also measure the dissipation $-s_e[\mathcal{C}_n]/k_B$ for each path $\mathcal{C}_n$. To resolve the relationships among precision, time resolution (speed), and dissipation, we generate an ensemble of paths conditioned on time, averaging observables over the set of paths that occur, $\langle \tau \rangle_{\mathcal{C}_n}$, within time intervals of uniform length, Δt.

Analyzing this model clock, we found that its timekeeping ability belongs to mode **I**. Figure 2(b) shows that, for the time-resolved ensemble of paths, the entropy dissipated, $-\Delta_e S_t/k_B$, is inversely related to the speed of path completion, $\langle 1/\tau \rangle_t$. We also see that the precision increases with the speed, Fig. 2(b). That is, the clock operates more precisely and with less dissipation by increasing the time resolution (path speed). At this level of description, faster paths are more precise and dissipate less, which is consistent with observations of other classical clocks.[37,38] This observation suggests that we can experimentally tune the temperature and voltage difference to increase the resolution (speed), $\langle 1/\tau \rangle_t$, and precision of timekeeping while simultaneously suppressing the dissipation, $-\Delta_e S_t/k_B$.

The correlation of these observables at the level of stochastic paths translates into our ability to optimize dynamical functions in practice by tuning experimentally controllable parameters. Exploring the parameter space, one would like to find regimes in which the time keeping is as accurate as possible (largest $\langle \tau \rangle^2/\sigma^2(\tau)$) with as little cost as possible ($-\Delta_e S/k_B$ closest to zero). We hypothesize from our calculations of path observables that these regimes are achievable by identifying parameters that weight the shortest paths (fewest transitions) in our ensemble averages, which are the fastest, most precise, and least dissipative. To test this hypothesis, we averaged all generated paths to compare across experimental conditions. Figure 2(c)

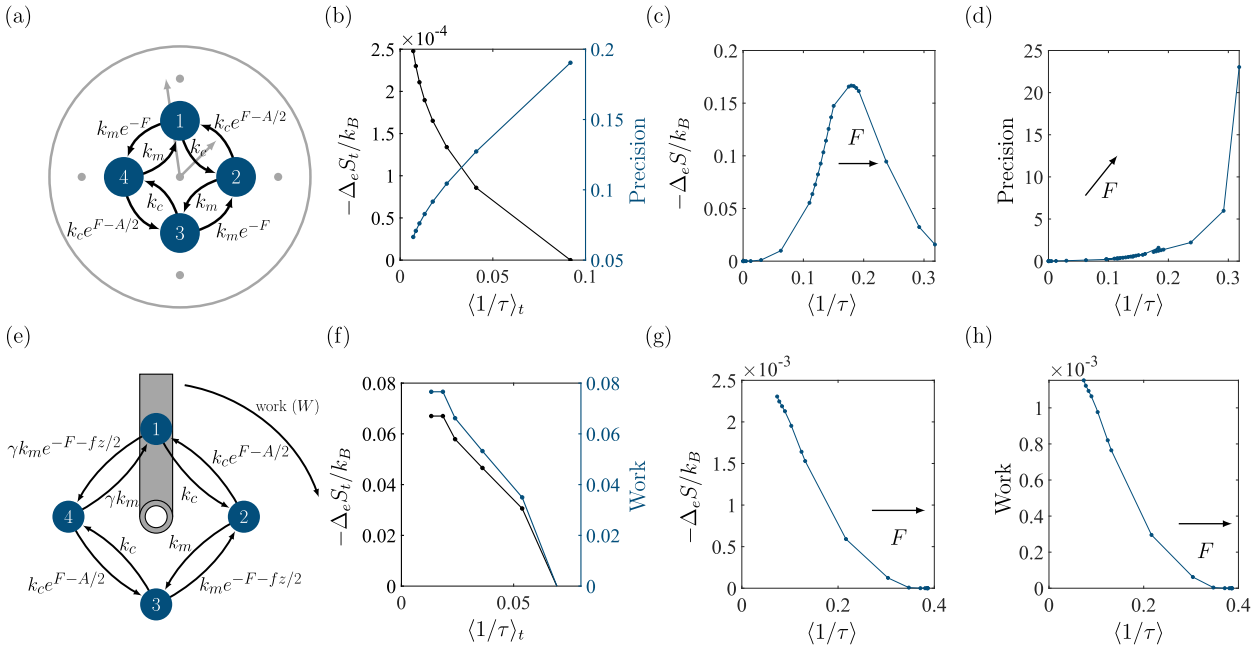

FIG. 2. Mode **I**: Faster stochastic paths enhance performance and suppress dissipative losses. (a) A four-state Markov model of a clock. (b) Time-resolved entropy dissipated $-\Delta_e S_t/k_B$ (left axis) decreases with the rate of path completion $\langle 1/\tau \rangle_t$. The precision of timekeeping $\langle \tau \rangle^2/\sigma_t^2(\tau)$ (right axis) increases with the rate of path completion. Each point corresponds to the subset of paths that occur in regularly spaced time intervals, $\Delta t = 0.5$. All model parameters are unity. (c) Entropy dissipated $-\Delta_e S/k_B$ and resolution (path speed) $\langle 1/\tau \rangle$ averaged over all paths upon varying the energy difference between electrodes F (blue) over values $F \in [0.1, 0.2, \ldots, 1, 2, \ldots, 10]$ with other parameters set to 1. (d) Over all paths in the ensemble, the precision $\langle \tau \rangle^2/\sigma^2(\tau)$ is a monotonically increasing function of the resolution $\langle 1/\tau \rangle$ when varying the energy difference between electrodes F, as in (c). Scanning F as we do here does not change the assignment of the function to **I**. Mode **II**: Slower stochastic paths enhance performance but also increase dissipative losses. (e) A four-state Markov model of a ratchet generating work through clockwise transitions. (f) Time-resolved ($\Delta t = 1.2$) entropy dissipated $-\Delta_e S_t/k_B$ (left axis) and work output $\langle W \rangle_t$ (right axis) tend to decrease with the rate of path completion $\langle 1/\tau \rangle_t$. Model parameters are $F = k_c = A = 1$ and $fz = 0.8$. (g) Over all paths in the ensemble, the entropy dissipated $-\Delta_e S/k_B$ decreases with $\langle 1/\tau \rangle$ when varying the energy difference between electrodes $F \in [0.1, 0.2, \ldots, 1, 2, \ldots, 10]$ with other parameters set to 1. (h) The work output W decreases with increasing speed $\langle 1/\tau \rangle$, varying the energy difference between electrodes F, as in (g).

shows the effect of the energy difference between electrodes, F, an experimentally controllable parameter, on the resolution (speed), $\langle 1/\tau \rangle$, and dissipation, $-\Delta_e S/k_B$. The total magnitude of the entropy dissipated (over the ensemble of paths completing at any time) is smallest when the magnitude of the energy difference between electrodes is large, with no preference for which electrode has a larger energy (large $|F|$), when the particle has approximately no charge ($A \approx 0$), and when the particle charge does not change ($k_c = 0$) or changes rapidly (large k_c).

Our numerical calculations also show that both the precision and the resolution (speed) are highest when the affinity is small (achieved at high temperatures), charges change quickly (k_c is large), and the energy difference between electrodes is large (F is large and positive), Figs. 2(c) and 2(d). The shortest paths effectively dominate the ensemble averages under these conditions, confirming our hypothesis. Thus, for the fastest, most precise, and most entropically efficient measurement of time, charge transfer k_c and particle motion k_m must be fast, electrodes should have a large energy difference F, and the affinity A should be as small as possible, Figs. 2(c) and 2(d). From these data, we can distill out the features associated with the first mode in our classification: resolution/speed improves precision and suppresses dissipation, and we can simultaneously extremize all three observables.

An immediate question is whether this mode **I** is specific to this model or, more generally, for timekeeping. Based on our survey of models so far, it seems unlikely that all clocks belong to this mode. We have found that not all models that belong to this mode are clocks. For example, we analyzed a model of nonequilibrium self-assembly[17] and found that it belongs in this mode of optimization (see supplementary material Fig. 10). Our findings here show that the optimization modes in Fig. 1 are for each model rather than each function. We also analyzed Markovian networks consisting of linear chains of states with randomly sampled transition rates, "Network features controlling modes of dynamical function models." However, we could not assign any of these models to **I** or **II**, suggesting that models for these modes need to be carefully and intentionally designed.

B. Slower stochastic paths enhance performance but also increase dissipative losses

Not all processes have paths that occur on short timescales with high efficiency. Another modality is possible in which we can

simultaneously optimize speed and dissipation at the expense of deteriorating functional performance. In this case, speed/dissipation and speed/performance are both negatively correlated, **II** of Fig. 1.

As an example of mode **II**, we consider a model ratchet. Power output is an important deliverable for many practically important systems.[39] Modified ratchet models can represent the transport of materials in cells via molecular motors.[8,40,41] Like the clock, our example model for this mode represents an electromechanical oscillator, but one that operates with an applied load to generate work.[1] The applied load adds three model parameters: an applied load f, a period z, and a dimensionless directionality parameter $\gamma = 0.001$. With these additional parameters, one revolution around the cycle of states can deliver work in the preferred direction $W_{\mathcal{C}_n} = fz$ and takes an amount of work $W_{\mathcal{C}_n} = -fz$ in the non-preferred direction. We consider paths that start and end in state 1, $x_0 = x_f = 1$, generating a fixed amount of work, $\pm fz$, for each path traversing the cycle. The work done is $W = fz$ for each clockwise revolution; work is done on the system, rather than by the system, $W = -fz$ if the system completes one revolution in the counterclockwise direction.

Analyzing the path space for this model ratchet, we find that slow paths tend to generate more work output but also produce more dissipation. The path speed is the mean speed, $1/\langle\tau\rangle_{\mathcal{C}_n}$, where the average here is over the trajectories taking the path. On average, fast paths have a shorter path length (the number of transitions along the path, n), supplementary material Fig. 2(b). As we found for the clock, fast paths dissipate less than slow paths, Fig. 2(f). However, these fast paths also tend to result in less work, Fig. 2(f). There are then two competing objectives for optimizing the functionality of this model: one can either aim to operate slowly to accomplish more work and pay the price of a large amount of dissipation, or one can aim to operate quickly to minimize the dissipation (to the extent possible) at the expense of delivering less work.

Averaging observables over the ensemble of paths, we found that it is possible to increase both power and speed while suppressing dissipation by tuning the working conditions of the ratchet. The clock and ratchet respond similarly in terms of speed and dissipation with respect to their common parameters: A, k_c, and F. As shown in Fig. 2(g), the speed at which the ratchet operates is faster and the dissipation is less when the affinity is small $A \approx 0$, the rate of charge change k_c is large, and the energy difference between electrodes F is large and positive. Physically, these parameter regimes correspond to a particle with a small charge oscillating between electrodes with a large difference in energy and changing the sign of its charge quickly. However, because work and speed are negatively correlated, modulating the parameters to increase the speed and decrease dissipation will also suppress the work output, Figs. 2(g) and 2(h). This mode of optimization persists when varying all parameters of this model, Fig. 2(h).

Unlike the clock, the ratchet model here is an example of a system in which speed, dissipation, and performance cannot all be optimized simultaneously. However, not all systems that produce power necessarily belong to this modality. What determines the modality of a given model depends on the space of stochastic paths; for the two models so far, the fastest paths of the clock are also the most precise, but the fastest paths of the ratchet have the least work output.

C. Slower stochastic paths enhance performance and suppress dissipative losses

So far, we have seen two modalities where fast stochastic paths incur smaller dissipative losses. However, Markov models are possible in which faster paths have larger dissipative costs. In mode **III** of Fig. 1, the speed is positively correlated with dissipation but negatively correlated with performance. For this modality, we consider a system capable of replication (e.g., DNA transcription), represented by the Markov model,[1] as shown in Fig. 3(a). The model consists of nucleotide monomers and dimers with concentrations c_m and c_d, respectively. A dimer of nucleotides can be correctly or incorrectly copied.[6,42] Like and unlike monomers interact with energies $\epsilon - \delta$ and ϵ and bind at rate B. The energy levels of these interactions have a difference of F. The performance of the copier is the ratio of the yield of the correct copy to the incorrect copy, [copy yield]/[miscopy yield]. The objective is to generate as much of the correct copy as possible or minimizing the amount of the incorrect copy.

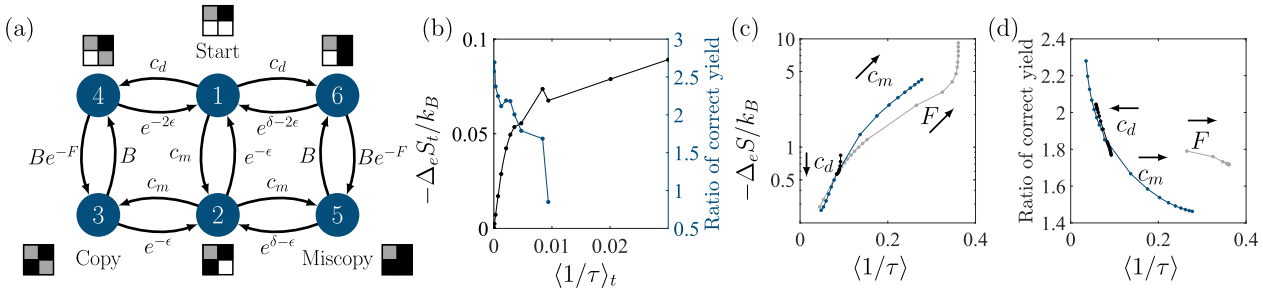

FIG. 3. Mode **III**: Slower stochastic paths enhance performance and suppress dissipative losses. (a) Diagram of a Markov model of DNA transcription. Monomers add to create a correct or incorrect copy of the initial dimer. (b) Time-resolved entropy dissipated (left, black) and ratio of correct yield vs speed (right, blue). Observable averages are over uniform-length time windows, $\Delta t = 1.75$. All model parameters are one. (c) Entropy dissipated vs speed with varying parameter values $\in [0.1, 1]$ with a step of 0.1 and $\in [1, 10]$ with a step of 1 for F (gray), c_d (black), and c_m (blue), and other parameters set to one. (d) Ratio of correct to incorrect yield vs speed with varying parameters values $\in [0.1, 1]$ with a step of 0.1 and $\in [1, 10]$ with a step of 1 for F (gray), c_d (black), and c_m (blue), and other parameters set to one.

To optimize this dynamical function, we analyze paths that start from the dimer ($x_0 = 1$) and end in either the correct copy ($x_f = 3$) or the incorrect copy ($x_f = 5$) of the dimer. Paths with a larger $1/\langle\tau\rangle_{\mathcal{C}_n}$ will quickly self-assemble structures and dissipate an amount of entropy, $-s_e[\mathcal{C}_n]/k_B$, the thermodynamic cost of the process. From our numerical calculations, paths with low $\langle 1/\tau\rangle_t$ generate a greater proportion of the correct copy and suppress dissipation, $-\Delta_e S_t$. Figure 3(b) shows that in the temporally coarse-grained ensemble of paths, increasing the path speed also increases the entropy dissipated. However, the proportion of the yield corresponding to correct copies decreases with increasing speed, $\langle 1/\tau\rangle_t$, Fig. 3(b). Put simply, expediting the copying process introduces errors, so there is an advantage to following slower stochastic paths in this model to ensure a high yield of correct copies and the suppression of dissipative losses.

Modulating parameters, we can find parameter regimes that optimize the performance of this copier over all paths completing at any time up to time t. We varied the concentration of the monomer c_m, the interaction energy between like monomers $\epsilon - \delta$, and the binding energy associated with the dimer B. Figures 3(c) and 3(d) shows that we can simultaneously increase the ratio of the correct yield and decrease the dissipation with these parameters. What improves the dynamical functionality is increasing the concentration of correct dimers (large c_d), decreasing the concentration of monomers (small c_m), and decreasing the energy difference between states (small F). However, these adjustments also decrease the speed of the process, $\langle 1/\tau\rangle$. So, slowing down the copier increases the ratio of correct yield and decreases the dissipative losses of operation. This trade-off is a consequence of the correlations between speed/dissipation and speed/performance in the temporally coarse-grained paths.

D. Faster stochastic paths enhance performance but also dissipative losses

The final modality, **IV** of Fig. 1, for dynamical functions has both dissipation and performance positively correlated with speed. One example of this modality is the Markov model of self-assembly[1] shown in Fig. 4(a). The model represents gold nanoparticles assembling into a tetrahedral structure,[43,44] which is characteristic of a larger class of systems in which there are efforts to design[45,46] subunits that autonomously form larger structures,[47] often out of equilibrium.[3,48] The nanoparticles can be in active or inactive forms, both of which can aggregate into a larger structure. The transition rates of the model depend on the concentrations of the assembled structure c_a and the monomer c_i, the kinetic rate constant for the driven k_a and undriven k_i processes, the interaction energy between monomers ϵ, the energy difference between levels F, and the affinity A.

As a measure of performance, we choose the yield of the fully assembled tetramer, which is the amount of the fully assembled structure $\sum_{t_0}^{t}\sum_{n=0}^{n_{\max}}\sum_{\mathcal{C}_n}\mu(\mathcal{C}_n, t)$ at a time t. We can directly measure the yield from the path probability $\mu(\mathcal{C}_n, \langle\tau\rangle_{\mathcal{C}_n})$ evaluated at the mean path occurrence time $\langle\tau\rangle_{\mathcal{C}_n}$. The paths here are those connecting $x_0 = 1$ and $x_f = 4$.

From our numerical calculations, the temporally coarse-graining observables show that the speed and entropy dissipation of paths exhibit a maximum, Fig. 4(b). Both the maximum speed and dissipation coincide with the maximum yield, Fig. 4(b). Maxima in dynamic yields have been observed experimentally in dissipative self-assembling systems driven by chemical reactions.[14] Here, the decline in speed and dissipation following the maxima is likely due to the maximum length of paths generated. To confirm, we increased the path length and saw that the average observable values converge. Because the path length and time required to complete a path are strongly linked, enumerating paths biases toward shorter, and therefore faster, paths, supplementary material Fig. 5. The paths included in our calculations are an accurate representation of the short-term behavior of interest here.

Unlike the clock and ratchet models, speed and dissipation are positively correlated in this model for self-assembly, [Fig. 4(b), left]. However, the nonequilibrium self-assembly model in Ref. 17 belongs to mode **I**, supplementary material Fig. 10. In that model, a positive correlation for speed/dissipation is only possible when the yield is negligibly small, meaning the function is not effectively accomplished. This result suggests that each model cannot change its mode of classification without also sacrificing its ability to perform its intended function. The distinct modalities of these models confirm that self-assembly is not restricted to mode **IV**, confirming that the protocol is assigning each *model*, not each *function*, to a given modality.

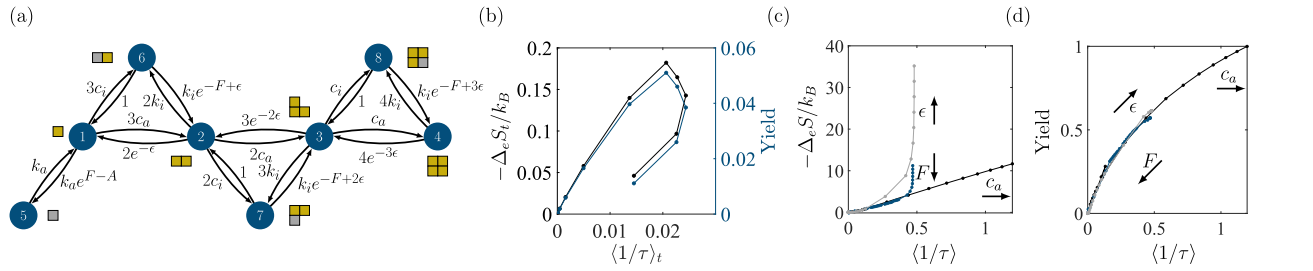

FIG. 4. Mode **IV**: Faster stochastic paths enhance performance but also dissipative losses. (a) Diagram of Markov model representing the self-assembly of gold nanoparticle tetramers. Progressing from left to right, monomeric units combine to create an assembled structure. Each monomer that adds can be in an active or inactive state. (b) Time-resolved entropy dissipated (left, black) and yield vs speed (right, blue). Averaging is within uniform-length time windows, $\Delta t = 0.5$. All parameters are one. (c) Entropy dissipated vs speed with varying each parameter p over values $p \in [0.1, 1]$ with a step of 0.1 and $p \in [1, 10]$ with a step of 1 for F (blue), c_a (black), and ϵ (gray), and other parameters set to one. (d) Yield is monotonically increasing with path speed when varying parameter values as in (c).

Figure 4(c) shows that while the binding energy, concentration of the assembled structure, and energy difference increase yield and speed simultaneously, they also increase the entropy dissipated. Panel (d) shows that high yields are possible on short timescales with large affinity $A \geq 1$, large monomer concentrations c_a and c_i, $\epsilon \geq 4$, lower energy for conformations of all active particles $F \leq -2$, and medial activation and deactivation rates $k_a \approx 1$ and $0.5 \leq k_i \leq 2$. Based on the relationships across the ensembles of paths, we can tune the parameters of this model to simultaneously optimize only two of the three observables of interest: we can increase the speed and yield, but only at the expense of dissipating more entropy.

1. Network features controlling the mode of dynamical function models

To identify the model features that affect the classification and optimization of their functionality, we analyzed both artificial[49] and designed networks. Applying the protocol, we can identify some emerging features of Markovian networks that determine their classification and optimization.

As a reference point and to systematically analyze the fluctuations in the transition rates over the network, we generated random networks of fully connected sets of $N = 4$ states with transition rates sampled from a Gaussian distribution with a mean of 5 and variances of 5, 10, 15, and 20. For our path analysis, we selected random initial and final states. These models are both fully connected and lack any systematic asymmetry in the forward/reverse transition rates, and we could consistently classify them as mode **IV** using either precision or yield as the performance metric. We see a positive correlation between speed and dissipation (faster paths generate greater dissipative losses) and between speed and performance (faster paths perform better in terms of either yield or precision).

In the four models for dynamical function here, the forward and reverse transition rates between two states are often unequal. When there is a net asymmetry in the transition rates around a cycle (e.g., the clock and ratchet models), there is the potential for more dissipation compared to the randomly generated models and the classification of a model as either (**I**, **II**) or (**III**, **IV**). To analyze the effect of this network feature on the classification, we introduced asymmetry into the rates of the fully connected models by instead sampling the rates from an exponential distribution with a mean of 10. In this case, the mode of these fully connected networks depends on the performance metric: **IV** using the yield and **III** using the precision. Imposing this amount of asymmetry on the network edges is insufficient to change the correlation between speed and dissipation, so modes **I** and **II** are still inaccessible. These results suggest that the performance metric is important in assigning the mode of a model for dynamical function, particularly when the forward and reverse transition rates are asymmetric.

Looking at the networks of the four models presented above, they also vary in their connectivity. To analyze this structural feature of the network, we generated networks of linear chains of three and four states on an energy gradient. Transitions downhill in energy have Arrhenius-like rate coefficients $e^{-\Delta\epsilon/k_BT}$, with $\Delta\epsilon = 100$ and $k_BT = 100$. Transitions uphill have a concentration dependence of $c = 0.1$, 1, 10, 100, and 1000. The mode of these linear networks again depends on the performance metric: **IV** using the yield and **III** using the precision. This assignment suggests that the performance metric can outweigh the network structure in determining the optimization of dynamical functions. However, this finding is not universal. For a single five-state cycle with forward (reverse) transition rates of 5 (1), the mode was **I** with both the yield and precision.

From our analysis of these random and designed models, what controls the classification is, in part, the structure of the network and its topological features (e.g., cycles and chains). For example, the presence of cycles is typically responsible for the negative correlation between speed and dissipation: traversing a cycle of states will have a net contribution to the entropy flow (when forward and reverse rates are unequal) and tend to delay the time to complete the function (when between the initial and final states). When there is a net-dissipative cycle, there is the possibility of a negative correlation between speed and dissipation, hence the assignment of the model as mode **I** or mode **II**. The distinction between mode **I** and mode **II** will depend on the correlation between the performance metric and speed, which is more dependent on the particular function and choice of metric.

The presence of a dissipative cycle or cycles is necessary but does not seem to be sufficient for classification as mode **I** or mode **II**. From our analysis of these random models, the cycle should also be a dominant feature of the network structure and its kinetics in order to affect the correlation between speed and dissipation. Otherwise, off-cycle transitions mask the dissipative losses in traversing the cycle and lead to a positive correlation between speed and dissipation. For example, the clock and ratchet models are both entirely composed of a single net-dissipative cycle, which is sufficient for a negative correlation between speed and dissipation and classification into mode **I** or mode **II**. However, the copier and self-assembling system belong to mode **III** or mode **IV**, despite having multiple net-dissipative cycles. These cycles constitute a smaller portion of the total structure of the network and are not sufficient for a negative correlation between speed and dissipation.

IV. CONCLUSIONS

Physical systems, whether living or synthetic, can function dynamically. To determine when these dynamical functions can be optimized for speed, we have mapped the design space by examining known, designed, and random models, including a Markov model clock, ratchet, self-assembling system, and copier. For a given set of external conditions, we view this design space from the perspective of the correlations between stochastic thermodynamic observables constrained by time across an ensemble of stochastic paths. These correlations determine the extent to which we can optimize the speed, performance, and dissipation of a dynamical function by tuning external conditions. The stochastic paths of dynamical functions show that optimizing the performance of their functionality depends on how the speed of these paths controls productive behavior and the dissipation of energy.

Our analysis also suggests a computational protocol to classify and design dynamical functions using stochastic thermodynamics. We demonstrated our protocol and each mode of optimization by examining known, designed, and random models of dynamical function, four of which span the design space of optimization modes: a clock, a ratchet, a self-assembling system, and a copier. Tuning external parameters, the models we analyzed here do not switch between modalities, except when they lose their ability to

actually function. Moreover, while each model belongs to a particular modality, other models of that function need not belong to the same modality; not all models for timekeeping will be more precise and less dissipative along faster stochastic paths. The protocol we propose is sufficiently general to apply to other Markov models of systems that function dynamically to determine to what extent we can optimize their speed, dissipation, and performance. Further applications could have implications for our understanding of the kinetics and thermodynamics of dynamical functions and the building of synthetic materials that accomplish functions on a specified timescale.

SUPPLEMENTARY MATERIAL

See the supplementary material for additional data and equations.

ACKNOWLEDGMENTS

This material is based upon work supported by the National Science Foundation under Grant No. 1856250. The work of R.A.B. was supported in part by the College of Science and Mathematics Dean's Doctoral Research Fellowship through fellowship support from Oracle, Project ID No. R20000000025727. The authors acknowledge helpful conversations with Erez Aghion.

AUTHOR DECLARATIONS

Conflict of Interest

The authors have no conflicts to disclose.

AUTHOR CONTRIBUTIONS

J.R.G. devised the project. R.A.B. and J.R.G. developed the theory. R.A.B. wrote the code. R.A.B. and J.R.G. analyzed results and wrote.

Rebecca A. Bone: Formal analysis (equal); Investigation (equal); Methodology (equal); Writing – original draft (equal); Writing – review & editing (equal). **Jason R. Green**: Conceptualization (equal); Funding acquisition (equal); Investigation (equal); Methodology (equal); Project administration (equal); Supervision (equal); Visualization (equal); Writing – review & editing (equal).

DATA AVAILABILITY

The data that support the findings of this study are available from the corresponding author upon reasonable request.

REFERENCES

[1]Y. Dou, K. Dhatt-Gauthier, and K. J. M. Bishop, "Thermodynamic costs of dynamic function in active soft matter," Curr. Opin. Solid State Mater. Sci. **23**, 28–40 (2019).
[2]R. Marsland and J. England, "Limits of predictions in thermodynamic systems: A review," Rep. Prog. Phys. **81**, 016601 (2017).
[3]S. Whitelam and R. L. Jack, "The statistical mechanics of dynamic pathways to self-assembly," Annu. Rev. Phys. Chem. **66**, 143–163 (2015).
[4]S. A. P. van Rossum, M. Tena-Solsona, J. H. van Esch, R. Eelkema, and J. Boekhoven, "Dissipative out-of-equilibrium assembly of man-made supramolecular materials," Chem. Soc. Rev. **46**, 5519 (2017).
[5]P. Sartori and S. Leibler, "Lessons from equilibrium statistical physics regarding the assembly of protein complexes," Proc. Natl. Acad. Sci. U.S.A. **117**, 114–120 (2020).
[6]S. D. McCulloch and T. A. Kunkel, "The fidelity of DNA synthesis by eukaryotic replicative and translesion synthesis polymerases," Cell Res. **18**, 148–161 (2008).
[7]A. C. Barato and U. Seifert, "Cost and precision of Brownian clocks," Phys. Rev. X **6**, 041053 (2016).
[8]R. Ait-Haddou and W. Herzog, "Brownian ratchet models of molecular motors," Cell Biochem. Biophys. **38**, 191–213 (2003).
[9]P. Xie, "Theoretical analysis of dynamics of kinesin molecular motors," ACS Omega **5**, 5721–5730 (2020).
[10]P. Pietzonka, A. C. Barato, and U. Seifert, "Universal bound on the efficiency of molecular motors," J. Stat. Mech. **2016**, 124004; S. Erbas-Cakmak, S. D. P. Fielden, U. Karaca, D. A. Leigh, C. T. McTernan, D. J. Tetlow, and M. R. Wilson, "Rotary and linear molecular motors driven by pulses of a chemical fuel," Science **358**, 340–343 (2017).
[11]I. Colomer, S. M. Morrow, and S. P. Fletcher, "A transient self-assembling self-replicator," Nat. Commun. **9**, 002239 (2018); M. Tena-Solsona, C. Wanzke, B. Rieß, A. R. Bausch, and J. Boekhoven, "Self-selection of dissipative assemblies driven by primitive chemical reaction networks," *ibid.* **48**, 7035–7039 (2018); X. He, R. Sha, R. Zhuo, Y. Mi, P. M. Chaikin, and N. C. Seeman, "Exponential growth and selection in self-replicating materials from DNA origami rafts," Nat. Mater. **16**, 993–997 (2017); M. R. D'Orsogna, G. Lakatos, and T. Chou, "Stochastic self-assembly of incommensurate clusters," J. Chem. Phys. **136**, 084110 (2012).
[12]R. Klajn, P. J. Wesson, K. J. M. Bishop, and B. A. Grzybowski, "Writing self-erasing images using metastable nanoparticle "inks"," Angew. Chem., Int. Ed. **48**, 7035–7039 (2009).
[13]B. Rieß and J. Boekhoven, "Applications of dissipative supramolecular materials with a tunable lifetime," ChemNanoMat **4**, 710–719 (2018).
[14]J. Boekhoven, W. E. Hendriksen, G. J. M. Koper, R. Eelkema, and J. H. van Esch, "Transient assembly of active materials fueled by a chemical reaction," Science **349**, 1075–1079 (2015); W. A. Ogden and Z. Guan, "Redox chemical-fueled dissipative self-assembly of active materials," ChemSystemsChem **2**, e1900030 (2020); S. Selmani, E. Schwartz, J. T. Mulvey, H. Wei, A. Grosvirt-Dramen, W. Gibson, A. I. Hochbaum, J. P. Patterson, R. Ragan, and Z. Guan, "Electrically fueled active supramolecular materials," J. Am. Chem. Soc. **144**, 7844–7851 (2022).
[15]A. Bupathy, D. Frenkel, and S. Sastry, "Temperature protocols to guide selective self-assembly of competing structures," Proc. Natl. Acad. Sci. U. S. A. **119**, e2119315119 (2022).
[16]C. Jarzynski, "Equalities and inequalities: Irreversibility and the second law of thermodynamics at the nanoscale," Annu. Rev. Condens. Matter Phys. **2**, 329–351 (2011).
[17]R. A. Bone, D. J. Sharpe, D. J. Wales, and J. R. Green, "Stochastic paths controlling speed and dissipation," Phys. Rev. E **106**, 054151 (2022).
[18]U. Seifert, "Stochastic thermodynamics, fluctuation theorems and molecular machines," Rep. Prog. Phys. **75**, 126001 (2012).
[19]L. Peliti and S. Pigolotti, *Stochastic Thermodynamics* (Princeton University Press, 2021).
[20]D. Helbing, "A contracted path integral solution of the discrete master equation," Phys. Lett. A **195**, 128–134 (1994); D. Helbing and R. Molini, "Occurrence probabilities of stochastic paths," *ibid.* **212**, 130–137 (1996).
[21]S. X. Sun, "Path summation formulation of the master equation," Phys. Rev. Lett. **96**, 210602 (2006); O. Flomenbom, J. Klafter, and R. J. Silbey, "Comment on "path summation formulation of the master equation," *ibid.* **97**, 178901 (2006); S. X. Sun, "Sun replies," *ibid.* **97**, 178902 (2006).
[22]H. Feng, B. Han, and J. Wang, "Dominant kinetic paths of complex systems: Gene networks," J. Phys. Chem. Lett. **1**, 1836–1840 (2010).
[23]N. Shiraishi, K. Funo, and K. Saito, "Speed limit for classical stochastic processes," Phys. Rev. Lett. **121**, 070601 (2018).
[24]G. Falasco and M. Esposito, "Dissipation-time uncertainty relation," Phys. Rev. Lett. **125**, 120604 (2020).

[25]S. B. Nicholson, L. P. García-Pintos, A. del Campo, and J. R. Green, "Time–information uncertainty relations in thermodynamics," Nat. Phys. **16**, 1211–1215 (2020).
[26]L. P. García-Pintos, S. B. Nicholson, J. R. Green, A. del Campo, and A. V. Gorshkov, "Unifying quantum and classical speed limits on observables," Phys. Rev. X, **12**, 011038 (2022).
[27]P. J. M. Johnson, M. H. Farag, A. Halpin, T. Morizumi, V. I. Prokhorenko, J. Knoester, T. L. C. Jansen, O. P. Ernst, and R. J. D. Miller, "The primary photochemistry of vision occurs at the molecular speed limit," J. Phys. Chem. B **121**, 4040–4047 (2017).
[28]D. T. Gillespie, *Markov Processes: An Introduction for Physical Scientists*, 1st ed. (Academic Press, 1991).
[29]M. F. Weber and E. Frey, "Master equations and the theory of stochastic path integrals," Rep. Prog. Phys. **80**, 046601 (2017).
[30]M. Manhart, W. Kion-Crosby, and A. V. Morozov, "Path statistics, memory, and coarse-graining of continuous-time random walks on networks," J. Chem. Phys. **143**, 214106 (2015).
[31]S. B. Nicholson, M. Alaghemandi, and J. R. Green, "Learning the mechanisms of chemical disequilibria," J. Chem. Phys. **145**, 084112 (2016).
[32]S. B. Nicholson, R. A. Bone, and J. R. Green, "Typical stochastic paths in the transient assembly of fibrous materials," J. Phys. Chem. B **123**, 4792–4802 (2019).
[33]R. Bone and J. Green (2022). "Contracted-paths," code is available at the Github repository. https://doi.org/10.5281/zenodo.6823402; (2022). "Dynamical-function," code is available at the Github repository. https://doi.org/10.5281/zenodo.6823319.
[34]J. M. Horowitz, "Diffusion approximations to the chemical master equation only have a consistent stochastic thermodynamics at chemical equilibrium," J. Chem. Phys. **143**, 044111 (2015).
[35]A. Coskun, M. Banaszak, R. D. Astumian, J. F. Stoddart, and B. A. Grzybowski, "Great expectations: Can artificial molecular machines deliver on their promise?," Chem. Soc. Rev. **41**, 19–30 (2012).
[36]A. C. Barato, "The cost of synchronization," Nat. Phys. **16**, 5–13 (2020).
[37]A. N. Pearson, Y. Guryanova, E. A. Laird, G. A. D. Briggs, M. Huber, and N. Ares, "Measuring the thermodynamic cost of timekeeping," Phys. Rev. X **11**, 021029 (2021).
[38]P. Pietzonka, "Classical pendulum clocks break the thermodynamic uncertainty relation," Phys. Rev. Lett. **128**, 130606 (2022).
[39]M. Esposito, K. Lindenberg, and C. Van den Broeck, "Universality of efficiency at maximum power," Phys. Rev. Lett. **102**, 130602 (2009).
[40]B. Alberts, A. Johnson, J. Lewis, D. Morgan, M. Raff, K. Roberts, P. Walter, J. Wilson, and T. Hunt, *Molecular Biology of the Cell*, 6th ed. (W. W. Norton, 2017).
[41]H. Wang and G. Oster, "Ratchets, power strokes, and molecular motors," Appl. Phys. A **75**, 315–323 (2002).
[42]Y. Song and C. Hyeon, "Thermodynamic cost, speed, fluctuations, and error reduction of biological copy machines," J. Phys. Chem. Lett. **11**, 3136–3143 (2020).
[43]R. Klajn, K. J. M. Bishop, and B. A. Grzybowski, "Light-controlled self-assembly of reversible and irreversible nanoparticle suprastructures," Proc. Natl. Acad. Sci. U. S. A. **104**, 10305 (2007).
[44]D. Manna, T. Udayabhaskararao, H. Zhao, and R. Klajn, "Orthogonal light-induced self-assembly of nanoparticles using differently substituted azobenzenes," Angew. Chem., Int. Ed. Engl. **54**, 12394–12397 (2015).
[45]S. Hormoz and M. P. Brenner, "Design principles for self-assembly with short-range interactions," Proc. Natl. Acad. Sci. U. S. A. **108**, 5193–5198 (2011).
[46]M. Nguyen and S. Vaikuntanathan, "Design principles for nonequilibrium self-assembly," Proc. Natl. Acad. Sci. U. S. A. **113**, 14231–14236 (2016).
[47]B. A. Grzybowski, C. E. Wilmer, J. Kim, K. P. Browne, and K. J. M. Bishop, "Self-assembly: From crystals to cells," Soft Matter **5**, 1110–1128 (2009).
[48]J. L. England, "Dissipative adaptation in driven self-assembly," Nat. Nanotechnol. **10**, 919–923 (2015).
[49]J. M. Horowitz and J. L. England, "Spontaneous fine-tuning to environment in many-species chemical reaction networks," Proc. Natl. Acad. Sci. U. S. A. **114**, 7565–7570 (2017).